Statistical analysis of meteoroid fragmentation during the Geminid and Leonid meteor showers

Narwa Rakesh Chandra[a*], Bathula Prem Kumar[b], Ganji Yellaiah[b]

[a]Department of Physics, Aurora's Engineering college, Bhongir, Hyderabad, Telangana 500 095, India

[b]Department of Astronomy, Osmania University, Hyderabad, Telangana 500 007, India

The meteoroid disintegration mechanism is a subject of interest as they are the sources for metallic layers in MLT region, ionspheric sporadic E, Noctilucent clouds and other aeronomy. It is known that meteoroid mass is deposited in the upper atmosphere either through fragmentation or through differential and simple ablation mechanisms. Each mechanism deposits the flux in different form (dust/ smoke-fragmentation, atomic form-ablation). Both the Leonid Meteor Shower (LMS) (parent body-Comet 55P/ Tempel - tuttle) and Geminid Meteor Shower (GMS)(parent body Asteroid- Phaethon 3200) are observed using MST Radar at NARL, Gadanki (13.5°N, 79.2°E). The atmospheric sodium density during the Geminid Meteor shower (GMS) is estimated using co - located sodium LIDAR. The ablation and fragmentation mechanisms of the meteoroid influx during these showers are studied using RTI plots from In phase and Quadrature channels of MST Radar, Signal to Noise Ratio (SNR) by estimating moments and line of sight velocities.

Our observations using MST Radar disclosed an important outcome that the asteroid originated meteoroids (Geminids) are undergoing less fragmentation when compared to comet originated meteoroids (Leonids). The fragmentation percentage estimated during the GMS is 14 % which is significantly lower than 20%, estimated for LMS. During GMS using Na LIDAR, it is also observed that the concentration of metallic sodium in ionosphere E - Region increased on peak activity day compared to pre peak day.

The line of sight velocities plotted for down the beam echoes during the showers dominantly followed a smooth evolution in altitude and time, before and after the occurrences of SNR changes, indicating that the meteoroids did not undergo any abrupt physical modification such as fragmentation. Further enhancement of atomic Na concentrations in E - region ionosphere during the shower indicates the flux deposition due to ablation.

After comparison it is found that the dominant meteoroid disintegration mechanism for Geminids is likely the ablation unlike the LMS.

We speculate here with substantial evidence that the contribution of fragmenting meteoroids in differently originated meteoroid showers is different and may be attributed to the chemical composition of their parent bodies of the meteoroids from which they are originated. This outcome has importance of its own as their parent bodies are different, the former shower being asteroid originated and the later comet originated. These results will also contribute in improving current meteoroid single body/dust ball ablation models.

Keywords: *Meteors, Geminids, Leonids, Radar, LIDAR, Fragmentation, Ablation*

1 Introduction

Every day millions of meteoroids, the space debris (in mass range of 10^{-11}g-10^{-4} g) in copious trajectories enter the Earth's atmosphere at very high entry velocities, undergo rapid frictional heating by collision with air molecules and their constituent minerals subsequently vaporize depositing abundant mass in Mesosphere Lower Thermosphere (MLT) region[1,2]. From these trajectory measurements, meteoroids have been found to have many different orbits, some clustering in streams often associated with a parent comet and the rest of the meteoroids of arbitrary trajectories are sporadic. Many of meteoroid characteristics can be determined as they pass through Earth's atmosphere in their trajectories. The meteoroids undergo variety of processes during its flight and play a pivotal role while depositing the matter both in the form of plasma and neutral atoms which manifest layers of neutral metal atoms (Na, Fe, Ca etc.), sporadic E layers and meteoric smoke particles[3-6], Polar Mesospheric Summer Echoes[7-9]. They deposit the mass either due to fragmentation, flaring and simple ablation, or differential ablation. The bright and ionized trail (plasma) immediately surrounding the meteoroid is able to back scatter Very High Frequency (VHF) electromagnetic waves[10-11].

Corresponding author (E-mail: rakeshnarwa@gmail.com)

Radar scattering from this region of plasma surrounding the meteoroid appears as the meteor head echo as it travels with the meteoroid yielding the line-of-sight velocity[12].

The first observations of meteor head-echoes were dated back to early 1940s Hey[13-15] and their study received attention only in the 1990s, when they were sensed using the high-power large-aperture (HPLA) radars[12,16]. The radar meteors were detected as noise in the ionsospheric D region which was enabled by direct extension of incoherent scatter observations[17-18]. Since then, the studies gained momentum and could explore many of the meteoroid parameters viz., meteoroid velocities[19-20], mass flux[21-22] and radiants[23] with the aid of head-echo observations. Further, have determined the form that the meteoroid mass flux takes when it enters the earth's atmosphere[24-25]. Using the EISCAT 930 MHz UHF HPLA radar, provided the evidence of fragmentation in sub millimeter sized meteoroids[26]. As noted by Mathews[24] in presenting fragmentation results from Arecibo, from the reports of Elford and Campbell[27] and Elford[28] it is understood that fragmentation is dominant in classical HF/VHF low-power small - aperture under dense (optically thin) meteor radar observations and is often interpreted in terms of over dense scattering. Fragmentation may transpire either because of thermally induced stresses[29-30] or because of the severance of a molten metal droplet from the lower density chondritic compounds of a heated meteoroid[31].

By adopting the meteor scattering analysis employed by the radar meteor scattering model detailed by Mathews *et al.*[32,33] and Mathews[34], fragmenting large meteoroids are observed by the Sondrestrom Radar Facility (SRF) 1290 MHz radar, only in the terminal phase of their encounter with the upper atmosphere. Dyrud and Janches[35] didn't find any evidence of meteoroid fragmentation in the vast majority of head echo observations at Arecibo 430 MHz UHF radar. However they also conclude that a simple ablation model cannot account for non smooth light curves observed by the radar. Roy *et al.*[36] followed similar scattering model and applied it to multiple head echoes and has attributed the light curves observed by Poker Flat ISR (PFISR) system to fragmentation. Janches *et al.*[37] attribute the non smooth meteor light curves observed by the Arecibo radar to differential ablation. Genge[31] reported that meteoroids during fragmentation, flaring and terminal processes,

while producing sufficient plasma to be radar visible, also directly produce nano meter dust or smoke particles as well as apparently many micrometeorites.

It is now believed that a meteoroid breaks up first because of the stress built up due to different aerodynamic forces exerted on different parts of the meteoroid. After the initial break up the aerodynamic interaction between the neighbouring fragments produce aerodynamic forces that push these fragments apart. The fragmentation continues and the fragments become smaller as the entry flight progresses and consequently decelerates faster.

2 The GMS and LMS

Asteroid (3200) Phaethon is a near-Earth asteroid (NEA) associated with GMS[38]. Phaethon's unusual orbit has a high inclination (i =22.18∘) and a very low perihelion distance (0.14 AU). Geminids is a major annual meteor shower which is interesting from several aspects because of its lowest orbital period of 1.5 years. Following the most recent taxonomy of DeMeo *et al.*[39], it is classified as a B-type object. Even after several investigations on the parent body[40] didn't found any measurable cometary activity classified Phaethon as an activated asteroid. Its reflectance spectrum suggests a connection with primitive meteorites, best fitting with CI/CM carbonaceous chondrites[41], aqueous altered and rich in hydrated silicates. Geminids is the only notable shower associated with asteroid 3200 Phaethon. J D Leon *et al.*[42] established a compositional and dynamical connection between two B-type objects: main belt asteroid and Pallas and near-Earth asteroid (3200) Phaethon. Thus ruling out speculation of Phaethon being an extinct comet[43].

The history of LMS is tied up with the development of the theory of meteor stream astronomy itself. The comet 55P/ Tempe 1 – Tuttle having a periodicity of 33 years undoubtedly is the parent body of Leonid meteor shower, the radiant of the shower located in constellation Leo with its RA at $10^h 08^m$ and Declination +22°. The comet had its recent perihelion passage in February 1998. The LMS is discussed thoroughly in Chandra *et al.*[44] and the references there in.

We know that the meteoroids deposit their mass in the Earth's atmosphere either through fragmentation or ablation. There are earlier reports of meteoroid fragmentation, fragmentation in head echoes[45] and specular trails[46-47] but till now a little or no work has been done to study the differences in fragmentation of meteoroids associated with showers originating from a comet and an asteroid. The work presented here

Table 1 — Radar parameters for meteor observations.

Frequency	53 MHz
Aperture area	16,900 m^2
Peak power	2 MW
Beam width	3°
Inter pulse period	1000 μs
Pulse width	8 μs
Altitude range	80–120 km
Number of coherent integrations	4
Fresnel zone length (at 100 km)	~5.32 m

brings out the differences in fragmentation of meteoroids associated Cometary originated Leonids and Asteroid originated Geminids and speculate the cause for such discrepancies. The work presented here is the first of its kind. This study is more important and argues to treat the differently originated meteoroids to be treated differently as their mass deposition mechanism differs. These results play a vital role in improving current meteoroid disintegration/ablation models.

3 Observations

The GMS (2007, 2011 and 2014) and LMS (2007, 2010 and 2014) respectively are observed with Indian MST radar located at Gadanki (13.5°N, 79.2°E), operating at 53MHz. The Indian MST Radar is a powerful tool for making detailed observations of meteor echoes because of its high power, narrow, near vertical beams and high Pulse Repetition Frequency. The MST Radar system description and technical specifications are given by Rao *et al.*[48]. The observations were carried out throughout the nights of 16th to 19th of November and 11th to 14th of December for LMS and GMS respectively in the corresponding years. The raw data is recorded with four different beam orientations (E$_{20}$, W$_{20}$, Z$_x$, N$_{13}$ subscript 20 indicates 20° off Zenith angle and one beam N$_{13}$ for sporadic E produced during meteor shower) from 18:00 hours to 06:00 LT each night continuously. Using the IGRF model for 1985, it is estimated at Gadanki that 13° off Zenith beam in the direction of North enables the radar beam to point perpendicular to Geomagnetic field lines at 110 Km. The value of magnetic dip angle at 110 Km corresponding to 13°N off Zenith direction is 12.77°N Jain and Rangarajan, 1992[49]. By coherently averaging four successive In phase (I) and Quadrature (Q) samples for each range bin, a sampling interval of 4ms is obtained. The offline analysis of raw data for each night is done by separating the frames containing the meteor echo signatures and thus mean hourly rates were estimated.

Using the co-located Na LIDAR at NARL, Gadanki, the metallic sodium deposited during the shower was also observed. The LIDAR was operated at mean resonance wavelength of 589nm. The technical details and functioning of LIDAR is described thoroughly by Bhavani Kumar *et al.*[50].

4 Results and Discussion

We have calculated the hourly rate of meteor occurrence during the showers and out of these counted meteors, we have separated meteoroids which have undergone fragmentation (from RTI plots, Amplitudes, SNR plots and line of sight velocities) and then estimated total number of meteoroids fragmenting per hour, i.e. fragmentation percentage for each hour. We have also described types of meteoroid fragmentation observed. In this work, we also presented Na density profiles observed during GMS in the year 2007 using co - located Na LIDAR.

The characteristic differences in the back scattered signals from the ablating and fragmenting meteoroids are thoroughly discussed aided with RTI plots, SNR plots, Arbitrary amplitudes and by estimating the abrupt changes is line of sight velocities of down the beam echoes. Further different types of fragmentation are also discussed. In the later sections the statistics of fragmentation during the GMS and LMS are presented. The figures presented here are illustrative of ablating and fragmenting meteoroids recorded during both the showers in their corresponding years of observations.

Around 15,000 frames of data are obtained in each year and visually examined all events with sufficient attention to clearly isolate smooth or ablative and fragmenting events in each year during both the showers. The figures presented below are the representative events of the samples collected during both the showers. Down the beam echoes extending to several range bins are presented here. As long as the meteoroid generated plasma is at least two times greater than the background plasma, radar could detect it. Once the plasma density falls below this criterion the trails goes undetected. We discuss here each echo presented in Fig. 1 separately.

The RTI plot of back scattered signal from meteoroid, SNR, arbitrary amplitude and its line of sight velocity are shown in Figs 1(a), 2(a), 3(a) and 4(a) respectively. As observed in Fig. 1(a), beginning and terminating altitude of the echo is ~ 113 Km and ~92 Km respectively and the trail formation is noticeable at ~ 102 Km. In Fig. 3(a). the
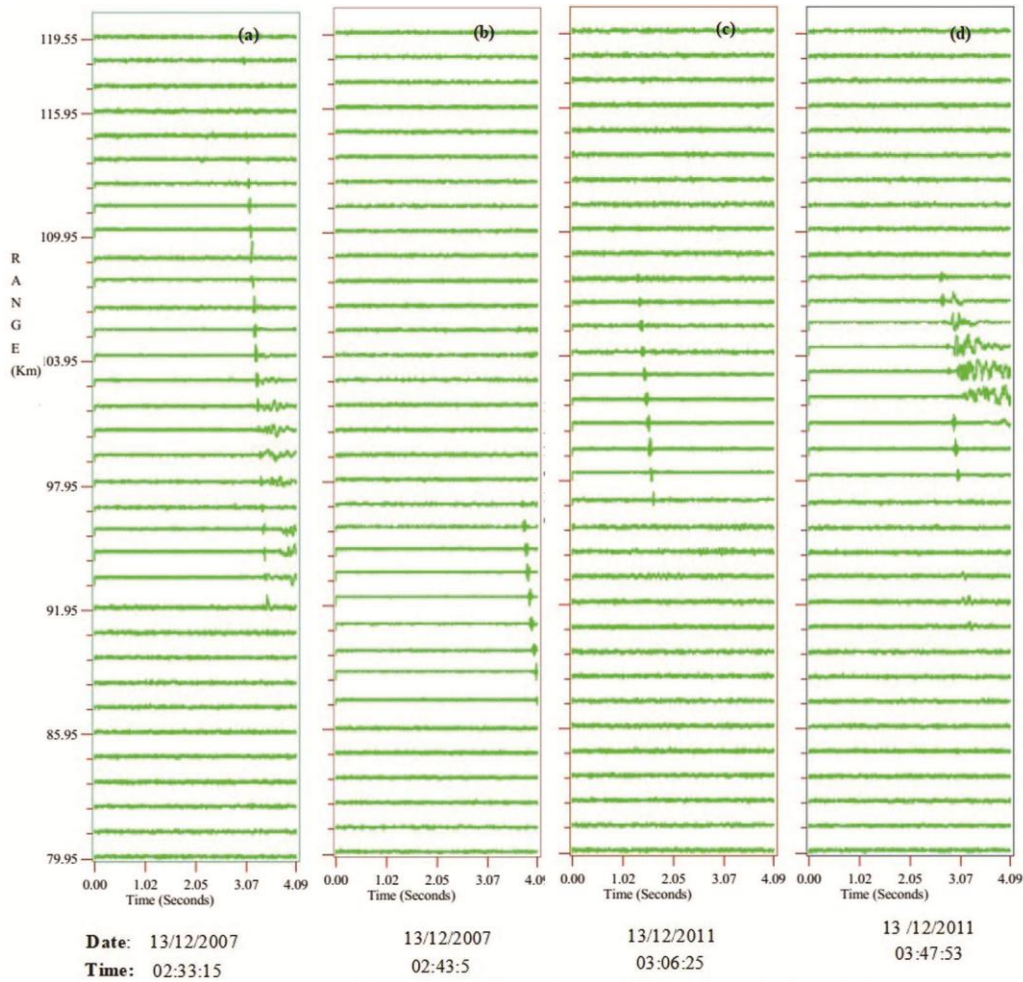
Fig. 1 — Meteor RTI plots observed during geminids 2007 & 2011.

radar detected echo after elapse of ~3 seconds and the trail formation is seen at ~3.3 seconds i.e., after a time lapse of fractions of second, (crests and troughs are noticeable). The sharp lines represent a head echo and thick crests and troughs represent the trail. The thick crests and troughs for a trail may be due to repeated constructive and destructive interference between back scattered signal from various portions of the trail. It can be noticed from the radar echo (Fig. 1(a) that even after the trail formation, the meteoroid has descended down without significant loss in velocity (the corresponding velocity plot is shown in Fig. 4(a). The remnant meteoroid which descended after the trail formation didn't create a trail and lost its mass due to ablation. It is known that during ablation and differential ablation, the velocity estimates follow a smooth evolution in altitude and time, before and after the changes in SNR this indicates that the meteoroid did not undergo an abrupt physical modification such as fragmentation[51-52]. The smooth increase of SNR

before these features is explained by considering the increase in electron production from a particle which is interacting with more and more air molecules, together with the fact that the particle is entering the higher transmitted power density region of the radar beam[53]. Thus, the steep changes in SNR must be related to a sudden increase or decrease in the rate of production of electrons giving rise to the meteor head plasma. During fragmentation, there will be a sudden change in velocities. This is evident that differential ablation is playing a role in meteoroid mass disintegration mechanism.

In Fig. 1(b), the head echo without trail is noticeable between ~95 Km and ~87 Km. The corresponding SNR and amplitude plots are shown in Figs 2(b) and 3(b) respectively. The SNR plot (Fig. 2 (b) shows a smooth variation in the received signal. In the Fig. 3(b), during the last quarter of the signal, after the elapse of ~3.7 sec, the sharp thin lines recorded here speaks about the head echo without any
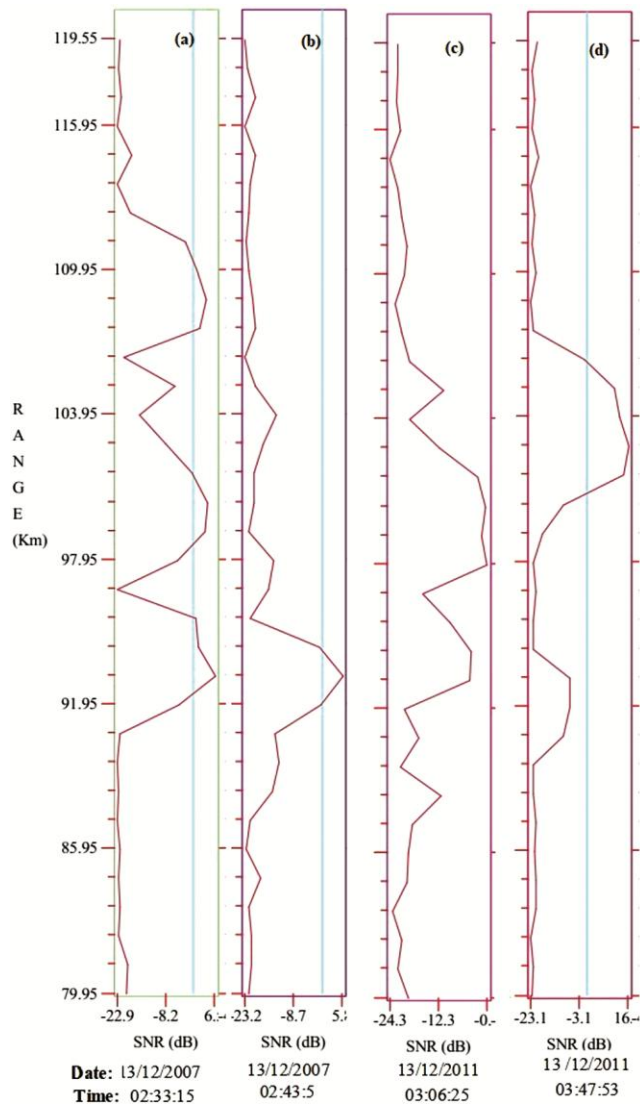
Fig. 2 — SNR plots of the echoes presented in Figs 1(a) – 1(d) respectively.

trail formation. From Fig. 4(b) it can be inferred that neither the trajectory of the meteoroid is altered during its flight nor there is any abrupt change in its velocity. The absence of such abrupt changes in the observed SNR plots and uniform velocity during its descend making it unlikely for fragmentation.

The meteoroid detection and disappearance heights are ~105Km and 96Km respectively in Fig. 1(c). The echo in Fig. 3(c) may be seen after the elapse of ~1.3 sec and lasted for 0.3 sec and terminated at ~1.6 sec. There are no evidences of trail formation and fragmentation and the echo has disappeared smoothly. The SNR plot as shown in Fig 2 (c) shows the bumps (the increase and decrease in SNR). These bumps may be due to back scattered signal from the uneven

ionization regions of the meteor or the increase/decrease in electron production from a particle which is interacting with more and more air molecules[53]. The rise and fall in power at different altitudes may be attributed to the constructive and destructive interference between back scattered signal from gradients of the plasma surrounding the echo. Fig. 4(c) shows a uniform velocity throughout the flight of the meteoroid till it vanished completely. Further, the smooth evolution in SNR and velocity plots makes this event a candid for meteoroid ablation.

Fig. 1(d) is a typical example of fragmentation. The meteoroid is detected at an altitude of ~ 107Km. After descending through a couple of range bins the meteoroid has fragmented. Figure 2(d) shows a dual peak in SNR, the first peak at 103Km and second at 92Km. In Fig. 3(d), the echo is seen after a lapse of 2.6 sec. and there is no trail formation till 2.8 seconds. The ablation has taken place in two phases. After fragmentation, the remnant part has descended down while the first part has generated a trail, thus they both existed simultaneously. The first fraction of the meteoroid undergone ablation initially and generated trail, the remnant part of it has gone undetected in the radar beam for few range bins and reappeared with the change in trajectory and was detectable till it disintegrated completely. Such evolution of the plasma associated with head echo is evident in the SNR plot (Fig. 2(d)) where there is a smooth increase in SNR as long as the ablation occurred and the SNR decreased when the remnant meteoroid has gone undetected. Further, with plasma rise associated with the head echo ablation the SNR has increased and was detectable for radar till it ablated completely. In the Fig. 3(d), it can be observed that the radar returns from the head echo is weak (at ~2.6sec) might be the head echo has entered the lower power density regions of the beam. The radar reflections from the trail are stronger than the head echo which is evident from the Fig. 3(d). After a lapse of fraction of second, the trail has formed and the observed crests and troughs are attributed to the constructive and destructive interference between the back scattered signal from various portions of the trail. Also further, the heat transferred to the meteoroid is to be distributed over the whole surface. For this to be strictly true, the meteoroid would have to be rapidly and randomly rotating. While it is unlikely that a meteoroid would be tumbling freely rapid rotation of the body is likely Hawkes & Jones[54]. If the body is rotating slowly or if the axis of rotation is parallel to
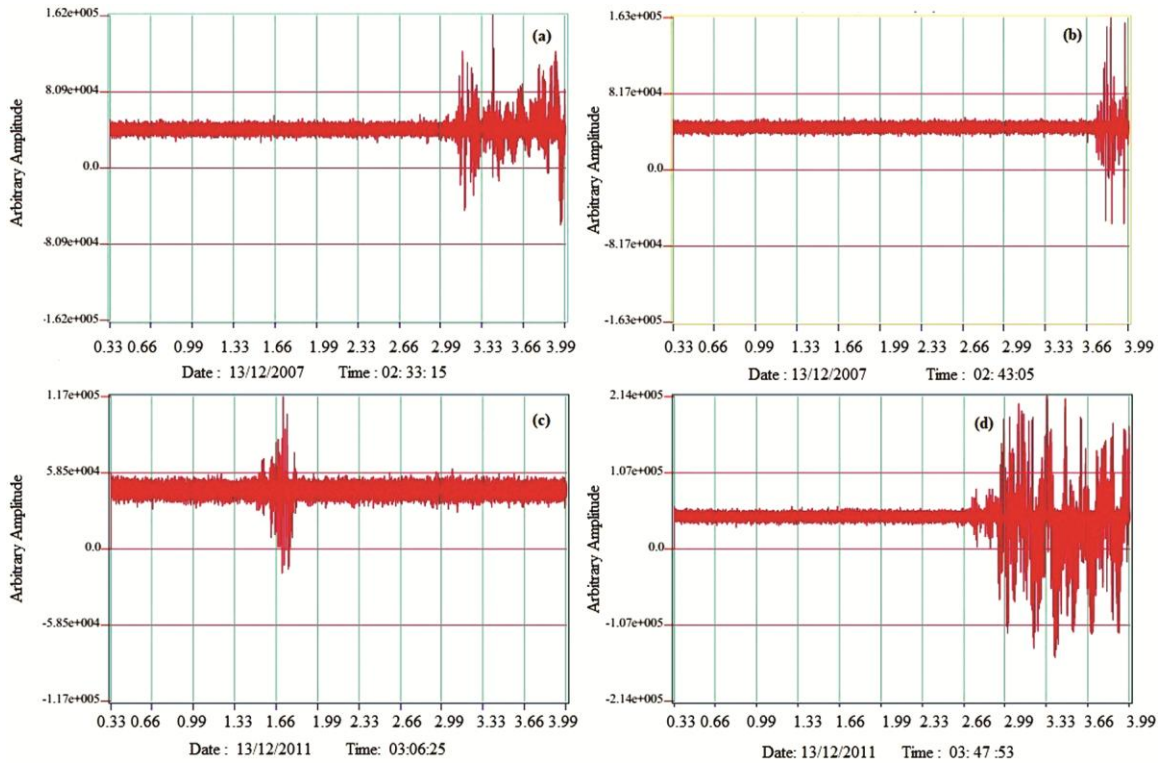
Fig. 3 — The arbitrary amplitudes of the meteor echoes presented in Figs. 1(a), (b), (c) and (d) respectively.

the direction of travel, only the front surface will be heated by the atmosphere. And as the radar detects this plasma generated during ablation, the absence of back scattered signal for few range bins may be because of this. Figure 4(d) shows an abrupt change in velocity and also in the trajectory. Such abrupt changes in the observed SNR plots and uniform velocity during it's descend makes it likely for fragmentation

Line of sight velocities

The line of sight velocities are estimated during the meteoroid flight for each range bin for the events presented above. The velocities of all the events are plotted with respect to their altitudes and are presented in Fig. 4. The smooth evolution of velocities is an index of ablation and differential ablation; this is found in Figs 4(a) – 4(c). Abrupt change in velocity is seen in Fig. 4(d), this may be because of physical modification of the meteoroid. This evidence substantiate that the fragmentation has occurred only for one event and the rest of the events are non fragmenting.

Mass of the meteoroids

The meteoroid mass plays a vital role in determining the meteoroid mass deposition mechanism. For the meteoroids below the μgm size, the fragmentation is
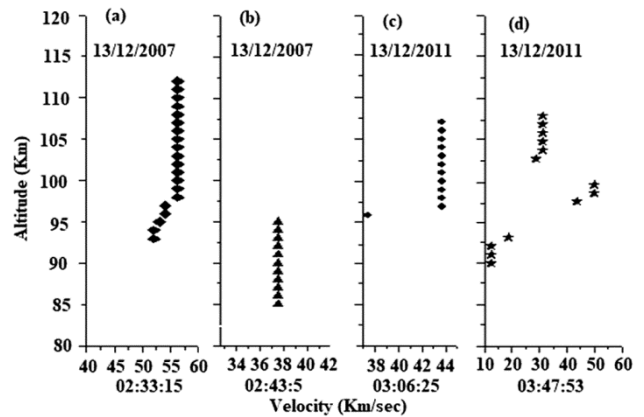

Fig. 4 — Line of sight velocities of the events presented in Figs 1(a) – 1(d) respectively.

not most likely pronounced. The meteoroids are likely to undergo the ablation and differential ablation. For examples presented above, the meteoroid mass is estimated using the method implemented by Jacobi and Stober[55]. The mass of the meteoroids are estimated and for the event presented in figure 1(d) and it is 1.18E-06 gm. For the events presented in Figs 1(a), (b) & (c) respectively are 5.1 E-08 gm, 9.72E-08gm & 4.58E-08gm. Thus the fragmentation is only possible in the last event 1(d). For the rest of the events the most plausible mechanism is ablation.
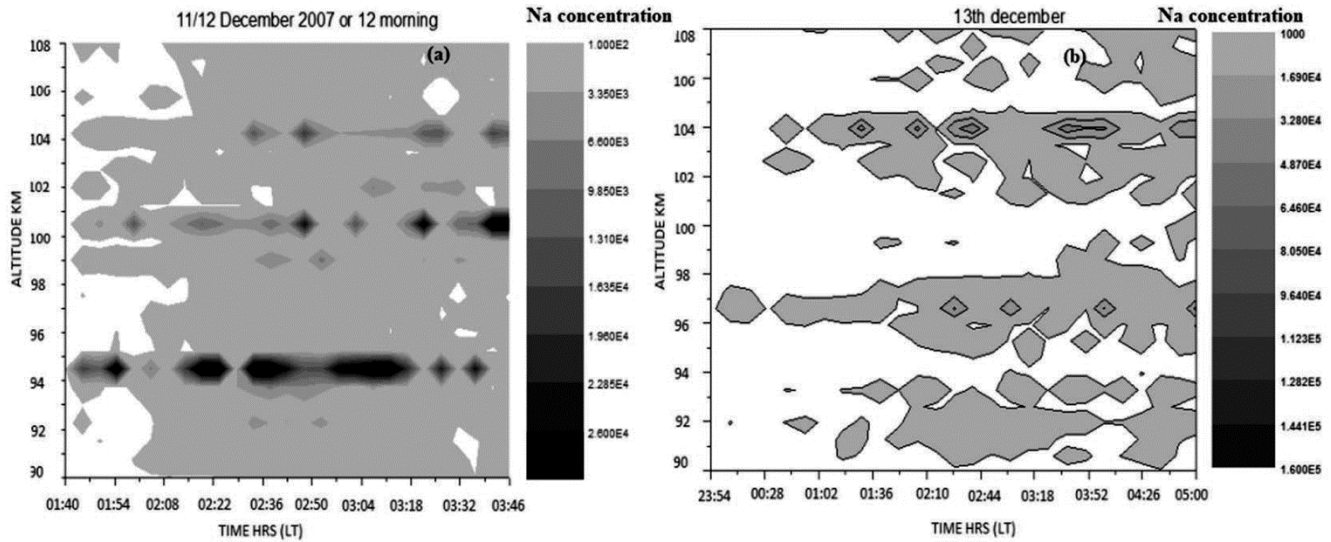
Fig. 5 — Na density profiles on (a) Pre Peak day (11/12 Dec) (b) Peak day (12/13 Dec).

Enhancement of metallic sodium layer

During the Geminid meteor shower 2007, the Na LIDAR was operated for few hours from 01:40 Hrs (LT) to 03:40 Hrs (LT) on 12th December and from 23:50 to 05:00 Hrs on 12/13th December. The LIDAR was operated for limited hours due to unclear and cloudy sky conditions. Thus the observations were only possible on pre peak day (11/12th December) and on peak day (12/13th December). The sodium density profiles for the above mentioned days are presented in Fig. 5. It can be inferred from the figure that during the peak hours (i.e. from 01:30 Hrs LT to 03:30Hrs LT) of activity on peak day (12/13th December), the sodium density is almost quadrupled during the same hours on pre peak day (11/12th December). The concentration of metallic sodium is increased by at least four times during the peak hours (comparing Figs 5(a) & (b)). The enhancement in the density of metallic Na layer during the Geminid shower manifests the physical modification mechanism that meteoroids have undergone to be either ablation or differential ablation. The enhancement establishes that, the mass deposition mechanism is dominated by ablation process over the fragmentation.

Types of fragmentation

Figures 6(a), (b) & (c) are typical examples of meteoroids undergoing simple fragmentation, continuous fragmentation and fragmentation in over dense trails respectively. As a case study we have presented here an example for each of the different kind of fragmentation that meteoroids have undergone during the showers.

Fig. 6(a) is a typical example of fragmentation in under dense specular radar meteor trail. The formation of such a specular radar meteor trail can be explained when the thin, relative to wavelength, meteor trail approaches the t_0 point (the point at which the trail is perpendicular to the radar pointing direction) the power received by the radar increases and continues to increase as the trail passes the t_0 point due to scattering from trail components lying within one Fresnel zone (length of one Fresnel zone is $(R_o\lambda/2)^{1/2}$ where, R_o is the range and λ is the radar wavelength) on either side of the t_0 point adding coherently. As the trail expands beyond one Fresnel zone, the phase-path difference between the trail components begins to increase, resulting in out-of-phase scattering from these components, thereby reducing the net received power. The ensuing constructive and destructive interference leads to the formation of a power signature, characterized by Fresnel oscillations, as shown in Fig. 6(a).

Figure 6(b) is an example of continuous fragmentation. Continuous fragmentation occurs when the meteoroid continuously loses fragments much smaller than the size of the body. These fragments slowly separate and increase the length of the meteor wake. As the separation between the fragments increase, the relative phase between backscattered signals from different fragments is not uniform and hence resulting in out-of-phase scattering from these components, thereby reducing the net received power.

Figure 6(c) is a typical example of fragmentation in over dense trail. It is characterized by a rapid rise like an under dense echo, followed by a plateau region and
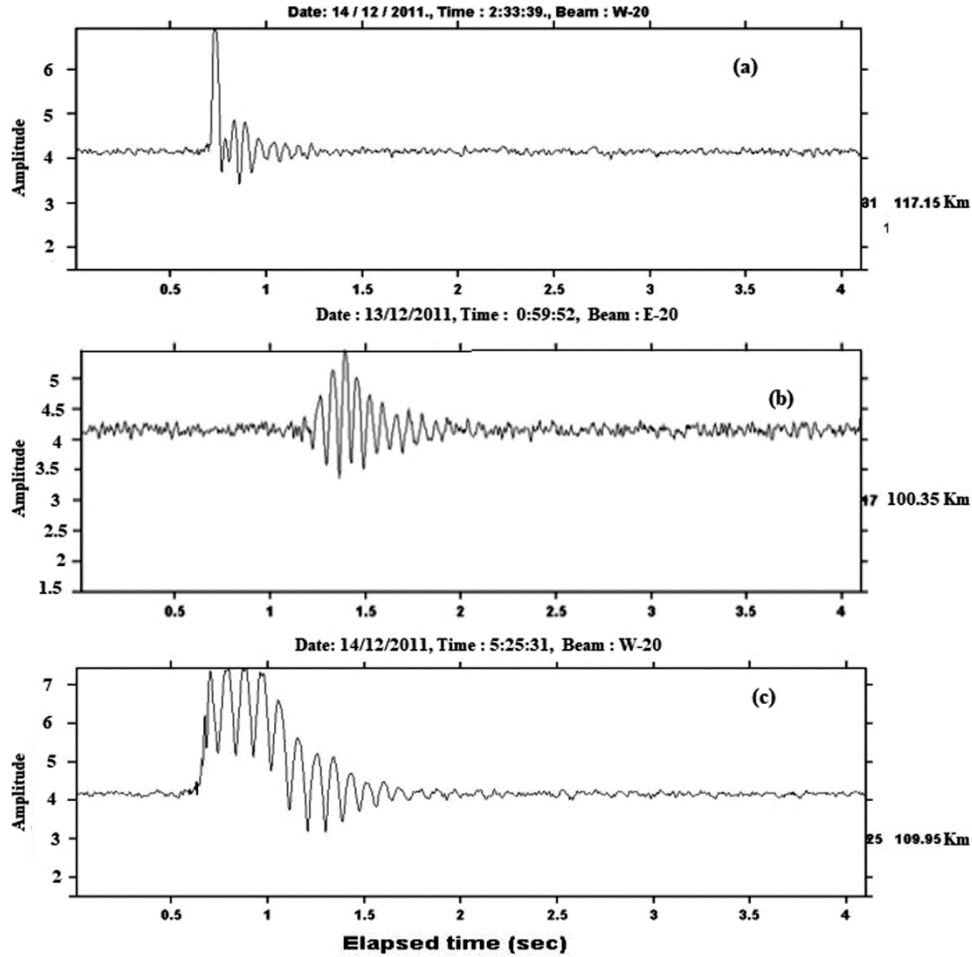
Fig. 6 — (a), (b) & (c) are the typical examples of meteoroid fragmentation.

then a steady decay in amplitude that tend to last for long, but in reality the trail is distorted by upper atmospheric winds and exhibiting multiple reflection points. The echo has commenced after 0.6s and the amplitude has reached to maximum and remained plateau for over 0.5 sec. This example shows short and strong enhancement in ionization at the moment of fragmentation, due to discharge of several small grains at once. The particles may be indeed single bodies and the anomalous structure of the ionization curves might be caused by chemical inhomogeneities or reflections from irregularities in the plasma surrounding the over dense echo[56]. The amplitude of over dense echo shows complex fluctuations with well defined signal strength, and later on, as the ionization diffuses, the over dense part gradually vanishes and the received power start decaying to background noise level like an under dense echo. The fast diffusion of the under dense part of this echo indicate that it occurred at higher altitude, and must have had very

large electron line density to remain over dense for over a duration of 1.5 s. From the range of detection, it can be expected that the echo was occurred at an altitude of 109.95 km.

The GMS is observed in the years 2007, 2011 and 2014 which occurs in the month of December and exhibits its peak activity from 11th to 14th of December. Even though the shower is monitored from 20:00 Hrs – 06:00 Hrs, the actual activity is assumed to begin after the rise of the radiant above the horizon. The shower has exhibited its maximum activity during the early hours of 13th December i.e. 02:00 Hrs – 04:00 Hrs (LT). Hence, the activity that was recorded after the midnight is only considered for studying the meteoroid fragmentation phenomenon. Table 2, shows the percentage of fragmentation and its mean during the Geminid and Leonid meteor showers from 00:00 – 06:00 Hrs LT.

On all the observation days it is noticeable from Table 2, that most of the meteoroids which are

Table 2 — Percentage of fragmentation.

Year	Day/ Time	00:01 - 01:00	01:00 - 02:00	02:00 - 03:00	03:00 - 04:00	04:00 - 05:00	05:00 - 06:00	Mean
Geminids								
2007	11/12	10.6	9.578	9.854	10.1428	8.555	11.56	10.0483
	12/13	12.785	12.817	13.625	13.125	12	11.675	12.6711
	13/14	10.071	12.5	12.5	11.2	8.7	9.2142	10.697
	14/15	10.727	10.455	12.637	10.91	11.546	10.476	11.1251
2011	11/12	8.02	16.6	6.08	9.7	10	9.4	9.9667
	12/13	11.8	12.38	10.09	21.5	20.5	14.4	15.11167
	13/14	7	13.4	13.8	14.2	13.8	12.24	12.40667
2014	11/12	13.4614	16.6666	15.85366	10	16.129	17.07317	14.86397
	12/13	11.1111	13.5135	14.7541	15.2542	13.253	22.78481	15.1117
	13/14	17.5	19.6969	10.1449	15.5555	16.8539	17.2413	16.1654
	14/15	9.0909	23.0769	18.6046	6.8965	12.9032	12.5	13.8543
Leonids								
2007	16/17	13.2857	12.571	15.2857	14.857	14	12.478	13.74623
	17/18	13.182	15.1	15.455	15.862	13.9128	11.565	14.1794
	18/19	12.75	14.125	14.25	14.125	17	13.375	14.27084
	19/20	15.533	12.988	14.433	15.54	12.2	8.53	13.204
2010	16/17	12.6	14.2	12.9	14.2	11.8	15.6	13.55
	17/18	16.6	17.6	20.5	23.3	20	20.8	19.8
	18/19	21.4	14.8	12	13.15	15.7	9.09	14.356
2014	17/18	16.21622	13.043	17.9104	11.3207	15.957	10.46512	14.152
	18/19	0	0	0	10.90909	34.42623	25.3968	23.577
	19/20	15.06	16.284	25	13.3333	21.875	16.6667	18.0365

undergoing fragmentation are recorded between 01:00 – 05:00 Hrs. The mean of fragmentation in Geminids meteoroids calculated for all the years is around 12.9%. In every year of observation during pre peak, on peak and post peak days, the fragmentation percentage is low, low, bettered and decreased again respectively on pre peak, on peak and post peak days respectively. This can be understood because the Earth might be entering the stream from the outer periphery, hence the Earth drags fewer number of meteoroids on pre peak day, on peak day the Earth is in the middle of the stream as a result it drags more number of meteoroids. And further, on post peak day the Earth leaves the stream hence the activity decreases. From Table 2, it is observed that large number of meteoroids have undergone fragmentation on peak day, compared to the other days. It is also known that fragmentation is a likely phenomenon for heavier meteoroids. As observed from Table 2, during the peak hours of activity on all the observation days, the percentage of fragmented meteoroids has increased and then gradually decreased. This shows that the Earth has encountered lighter particles of the stream first and then the heavier ones. Similar trend is also observed in the Leonids meteor shower, the estimated mean of fragmentation in Leonids meteoroids is around 16.1%.
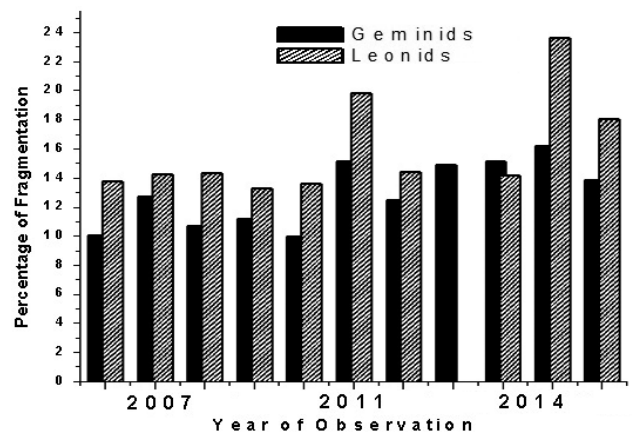

Fig. 7— Comparison of meteoroid fragmentation during the Geminids and Leonids meteor shower

The percentage of fragmentation on each shower day of Leonids and Geminids are presented in Table 2. The mean of fragmentation percentage on each day of observation during the Leonids and Geminids meteor shower in the years of observation is plotted in Fig. 7. It can be inferred from Fig. 7 that the Leonids has bettered in mean fragmentation percentage than Geminids. On all the observation days the fragmentation is minimal for Geminids when compared to Leonids. Geminid meteors are much more durable than typical cometary meteors: studies

of their ablation in Earth's atmosphere have shown that they have mean densities[57] of 2.9 g cm−3, the highest of any of the streams measured. This may imply that the Geminids are made of relatively strong rocky a steroidal material rather than more porous and fragile cometary material. The derived metallic abundances of 2004 Geminid meteor, especially Na/Mg depletion and excess Ni/Mg, show different features from other meteors whose parent bodies are comets[58]. The 3200 Phaethon from which Geminid meteor shower originates is classified as B – Type Asteroid because it is composed of dark material. The Leonid Meteor shower originating from Comet 55P/Tempel – Tuttle is rich in H, C, N, O, S and K, Ca. The temperatures attained by Geminid meteoroids are approximately 4000K while those attained by Leonid Meteoroids are 2500 – 3000K Jenniskens[59]. Comparing the relative chemical abundances of a Geminid meteoroid with those obtained from meteoroids associated with comet55P/Tempel–Tuttle and 109P/Swift–Tuttle, Rodr´ıguez *et al.*[58] found no significant chemical differences in the main rock forming elements. Despite this similarity, the deepest penetration of the Geminid meteoroids and their ability to reach high rotation rates in space without fragmentation suggested that thermal processing was affecting their physical properties.

Spectroscopy of B-class objects suggests major surface constituents of anhydrous silicates, hydrated clay minerals, organic polymers, magnetite, and sulfides. The constituents of comets are CO, CO_2, H_2O, NH_3, CH_3OH, CH_2OH, HCN.

Vojacek *et al.*[60] made Parallel double-station video observations of meteors and reported that all of the Iron-poor meteoroids have cometary Halley-type orbits (Leonids belong to the class of Halley type). Further Fe-poor meteoroids have low material strength, their beginnings of ablation are usually high. He also reported that Meteoroids with comet origin had heterogeneous composition, from Sodium -free, sodium -poor, and Iron-poor for Halley-type orbits. According to Borovička *et al.*[61] for Na depletion in these types of orbits might be the long exposure to cosmic rays on the comet surface during their residence in the Oort cloud. This process can lead to the formation of Na-free refractory crust. The gradual or sudden disintegration of the crust during the cometary passage through the inner solar system then produces millimeter-sized compact Na-free meteoroids. He also observed that some of the Geminid meteoroids are found to be Na rich, few are found to be depleted of Na. The explanation, as suggested by Borovička *et al.*[61] that the Na content is correlated with the age of the meteoroid. Younger meteoroids that have fewer passages close to the Sun retain more Na, which implies that the Geminid meteoroid stream was not formed in one instant. Alternate analysis of Borovička *et al.*[62]. suggested that differences in porosity may be the main reason of the differences in Na content in the Geminids. Vojacek *et al.*[60] also reported that most of the meteoroids on the asteroidal-chondritic orbits (Geminids) were found to be iron meteoroids.

From the above discussions it is notable that the comets are distinctly different from the asteroids in many ways and mostly in their chemical composition. An asteroid composition is different from that of a comet. Hence the cometary originated meteoroids chemically differ from the asteroid originated meteoroids. We speculate that as the chemical composition of differently originated meteoroids (comet – Leonid and asteroid – Geminid) is different from each other and hence the mass deposition mechanisms of both the meteoroids are different. More porous and less dense meteoroids (Leonids – cometary originated) are undergoing more fragmentation when compared to rocky and highly dense meteoroids (Geminids – Asteroid originated). We attribute our observation of high percentage of fragmentation of Leonids and low percentage of fragmentation in Geminids to the chemical composition of the meteoroids and their parent bodies. The differential ablation observed in Fig. 1(a) may be because of their ability to reach high rotation rates in space without fragmentation suggested that thermal processing was affecting their physical properties. Thus we propose that in determining the fragmentation not only the meteoroid mass has to be considered but also its chemical composition.

5 Conclusions

From the statistical analysis of Leonid and Geminid meteor showers, it is understood that the percentage of fragmentation is less pronounced for asteroid originated Geminids when compared to comet originated Leonids. The thermal exposure of objects in space plays a vital role in determining their physical and chemical properties. The asteroid 3200 Phaethon has an orbital period of ~1.5 years (comet 55P/Tempel – Tuttle, 33 years) and its closest approach is much shorter than 55P/Tempel – Tuttle,

hence its exposure to solar radiation is higher and frequent. Thus 3200 Phaethon has undergone more thermal treatment (frequent exposure results in loss of volatiles from the surface of the body). We attribute the differences in fragmentation of meteoroids during Geminid and Leonid shower to the difference in their chemical composition, high rotation rates and thermal exposure of parent object.

Acknowledgement

References

1   Janches D & Chau J L, *J Atmos Solar Terr Phys*, 67 (2005) 1196.
2   Mathews J D, Janches D, Meisel, D D & Zhou, Q H, *Geophys. Res. Lett.,* 28 (10) (2001) 1929.
3   Hunten, D M, Turco R P & Toon O B. *J Atmos Sci,* 37 (1980) 1342.
4   Kalashnikova, O, M. Hora ´nyi, G E Thomas & O B. Toon, *Geophys. Res. Lett.,* 27 (2000) 3293.
5   Plane J M C, *Chem Rev*, 103 (2003) 4963.
6   Saunders R W & Plane J M C, *J Atmos Sol Terr Phys*, 68 (2006) 2182.
7   Rapp M, Hedin J, Strelnikova, I, Friedrich M, Gumbel J & Lubken F, J *Geophys. Res. Lett.,* 32 (2005) L23821.
8   Bellan P M, *J Geophys. Res*., 11 3 (2008) D16215,
9   Rapp M & Lubken FJ, *Atmos. Chem. Phys,* 4 (2004) 2601.
10   Baggaley W J, *Meteors in the earth atmosphere, Cambridge University Press*, (2002) 123.
11   Stober G & Jacobi Ch, *Sci. Rep. Met. Inst. Univ. L.,* 41 (2007) 47.
12   Mathews J D, Meisel D D, Hunter K P, Getman V S & Zhou Q, *ICARUS*, 126 (1997) 157.
13   Hey J S & Stewart G S, *Derivation of meteor stream radiants by radio reflexion methods, Nature,* 158 (1946) 481.
14   Hey J S & Stewart G S, *Proc. Phys. Soc*., 59 (1947) 858.
15   Mathews J D, *J Atmos Sol Terr Phys*, 66 (2004) 285.
16   Pellinen-Wannberg A & Wannberg G, *J Geophys Res*, 99 (1994) 11379.
17   Mathews J D, Breakall J K & Ganguly S, *J Atmos Terr Phys*, 44 (1982) 441.
18   Mathews J D, *J Atmos Terr Phys*, 46 (1984) 975.
19   Janches D, Nolan M C, Meisel D D, Mathews J D, Zhou Q H & Moser DE, *J Geophys. Res*., 108 (2003) 1222.
20   Janches D J, Mathews J D, Meisel D D & Zhou Q, *ICARUS*, 145 (2000) 53.
21   Fentzke J T & Janches D, *J Geophys Res*, 113 (2008) A03304.
22   Mathews J D, Janches D, Meisel D D & Zhou Q H, *Geophys. Res. Lett.,* 28 (10) (2001) 1929.
23   Chau J L, R F Woodman & F Galindo, *ICARUS*, 188 (2007) 162.
24   Mathews S J, Briczinski A & Malhotra J Cross, *Geophys. Res. Lett.*, 37 (2010) L04103.
25   Malhotra A & J D Mathews, *A study on various meteoroid dis-integration mechanisms as observed from the Resolute Bay Incoherent Scatter Radar (RISR), Proceedings of Meteoroids 2010, NASA, Breckenridge, Colo.*
26   Kero J, Szasz C, Pellinen-Wannberg A, Wannberg G, Westman A & Meisel D D, *Geophys. Res. Lett.,* 35 (2008) L04101.
27   Elford W G & Campbell L, *Proceedings of the Meteoroids 2001 Conference, 6–10 August 2001, Kiruna, Sweden, ed. by Barbara Warmbein, ESA SP-495, (ESA Publications Division, Noordwijk,* (2001) 419.
28   Elford W G, *Atmos. Chem. Phys.,* 4 (2004) 911.
29   Jones J & Kaiser T R, *Mon.Not. R. Astron. Soc.,* 133 (1966) 411.
30   Verniani F, *J Geophys. Res.,* 78 (1973) 8429.
31   Genge M J, Engrand C, Gounelle M & Taylor S, *Meteoritics and Planetary Science Archives*, 43 (3) (2008) 497.
32   Mathews J D, Doherty J F, Wen C H, Briczinski S J, Janches D & Meisel D D, *J Atmos Sol Terr Phys,* 65 (10) (2003) 1139.
33   Mathews J D, Briczinski D, Meisel & Heinselman, *Earth Moon Planets,* 102 (1–4) (2008) 365.
34   Mathews J D, *J Atmos Sol Terr Phys*, 66 (2004) 285.
35   Dyrud L P & Janches D, *J Atmos Sol Terr Phys*, 70 (2008) 1621.
36   Roy A, Briczinski S J, Doherty J F & Mathews J D, *IEEE Geosci Remote Sens Lett,* 6(3) (2009) 363.
37   Janches D, Dyrud L P, Broadley S L & Plane J M C, *Geophys. Res. Lett.,* 36 (2009) L06101.
38   Whipple F L, *IAU Circ*, 62 (1983) 3881.
39   Demeo F E, Binzel R P, Slivan S & Bus J, *ICARUS,* (202) (1) (2009) 160.
40   Hsieh Henry H & David Jewitt, *The Astrophysical Journal,* 624 (2005) 1093.
41   Licandro J, Campins H, Mothe-Diniz T, Pinilla-Alonso N & de Leon, *J A & A,* 461 (2007) 751.
42   León J de, Campins H, Tsiganis K, Morbidelli A & Licandro J, *A & A*, 513 (2010) A26.
43   Peter Jenniskens, *Proc. 'Dust in Planetary Systems', Kauai, Hawaii, 2005 (ESA SP-643, January 2007).*
44   Chandra Rakesh N, Yellaiah G, Vijaya Bhaskara Rao S, *Indian J Radio Phys*, 40 (2011) 67.
45   Roy A, Briczinski S J, Doherty J F, Mathews J D, *IEEE*, 6 (2009) 363.
46   Patil A, Malhotra A, Patra A K, Prasad T R & Mathews J D, *Earth Moon Planets,* 114 (2015).
47   Yellaiah G & Chenna Reddy K, *Astrophysics and Space Science,* 361 (2016) 83.
48   Rao P B, Jain A R, Kishore P, Balamuralidhar P, Damle S H & Viswanathan G, *Radio Sci*., 30 (1995) 1125.
49   Jain A R & Rangarajan G K, *Scientific report 1SRO-NMRF-SR-37-92*, 1992.
50   Kumar Bhavani Y, Rao Narayana D, Sundaramurthy M & Krishnaiah M, *Optical Engineering*, 46 (2007) 086203.
51   Kero J, Szasz C, Pellinen-Wannberg A, Wannberg G & Westman A, *Earth Moon Planets*, 95 (2005) 633.
52   Mathews J D, Briczinski J, Meisel J & Heinselman J, *Earth Moon Planets*, 102 (1–4) (2008) 365.
53   Dyrud L P & Janches D, *J Atmos Sol Terr Phys*, 70 (2008) 1621.
54   Hawkes R L & Jones J P, *Mon. Not R astr Soc*, 185 (1978) 727.
55   Stober G, Jacobi Ch & Wiss. Mitteil, *Inst. f. Meteorol. Univ. Leipzig Band,* 42 (2008) 155.

56 Campbell-Brown M D & Close S, *MNRAS*, 382 (2007) 1309.

57 Babadzhanov, *A & A*, 384 (2002) 317.

58 Rodriguez T, Llorca J, Borovička J & Fabregat J, *Meteoritics & Planet Sci*, 38 (2003) 1283.

59 Jenniskens P, Rietmeijer F J M, Brosch N & Fonda M, *Leonid Storm Research*, *Springer-Science+Business Media, B.V.,* (2000) 321.

60 Vojáček V, Borovička J, Koten P, Spurný P & Štork R, *A & A,* (2015) 580.

61 Borovička J, Koten P, Spurný P, Boček, J & Štork, R, *Icarus*, 174 (2005) 15.

62 Borovička J, Koten P & Spurný P, *Proceedings IAU Symposium*, Issue S263 (Icy Bodies of the Solar System), (5) (2009) 218.